Chemical Research in Toxicology

Article

Effect of Subcellular Translocation of Protein Disulfide Isomerase on Tetrachlorobenzoquinone-induced Signaling Shift from Endoplasmic Reticulum Stress to Apoptosis

Zixuan Liu, Yawen Wang, Yuxin Wang, Wenjing Dong, Xiaomin Xia, Erqun Song, and Yang Song

Chem. Res. Toxicol., **Just Accepted Manuscript** • DOI: 10.1021/acs.chemrestox.7b00118 • Publication Date (Web): 20 Aug 2017

ACS Publications

Chemical Research in Toxicology is published by the American Chemical Society.
1155 Sixteenth Street N.W., Washington, DC 20036

Effect of Subcellular Translocation of Protein Disulfide Isomerase on Tetrachlorobenzoquinone-induced Signaling Shift from Endoplasmic Reticulum Stress to Apoptosis

Zixuan Liu, Yawen Wang, Yuxin Wang, Wenjing Dong, Xiaomin Xia, Erqun Song, Yang Song*

Key Laboratory of Luminescence and Real-Time Analytical Chemistry (Southwest University), Ministry of Education, College of Pharmaceutical Sciences, Southwest University, Chongqing, People's Republic of China, 400715

*Corresponding Author:

College of Pharmaceutical Sciences, Southwest University, 216 Tiansheng Road, Beibei, Chongqing, 400715 China

Tel: +86-23-68251503. Fax: +86-23-68251225

E-mail: songyangwenrong@hotmail.com

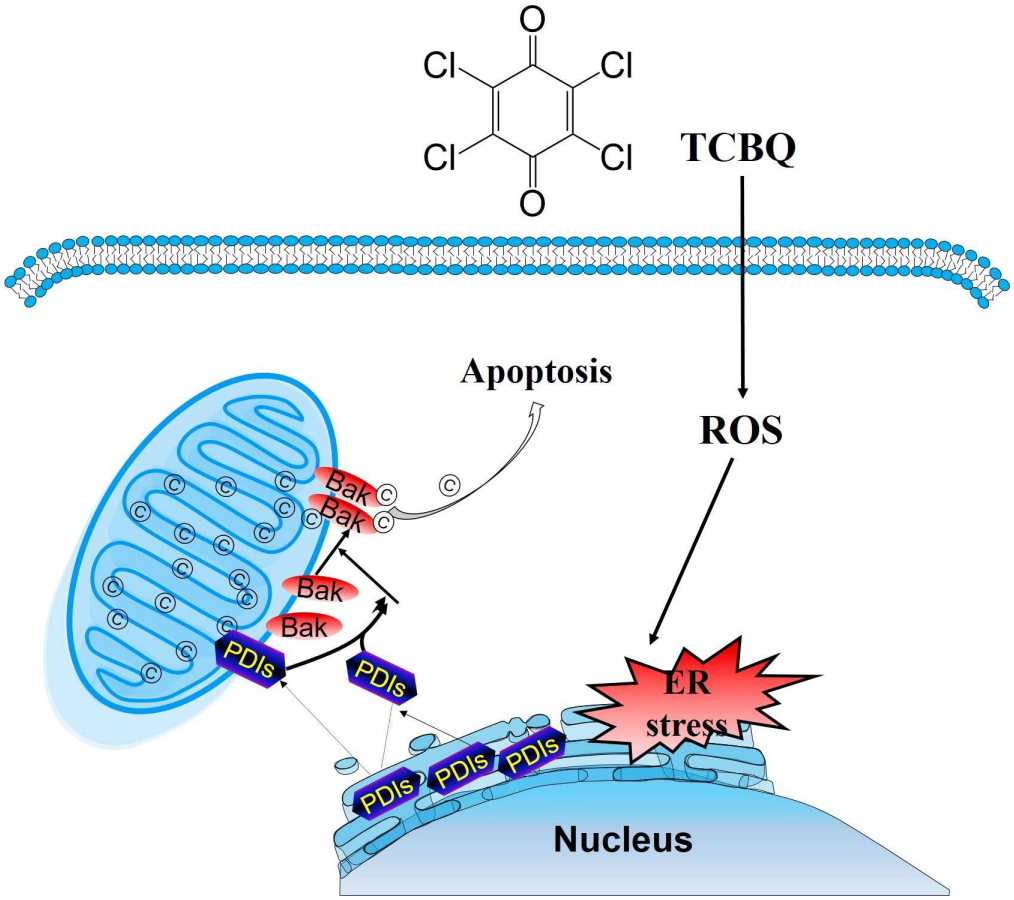
O
Cl
Cl
Cl
Cl
O
TCBQ
Apoptosis
ROS
Bak
Bak
Bak
Bak
PDIs
PDIs
ER
stress
PDIs
PDIs
PDIs
Nucleus

ABSTRACT

Our previous studies illustrated tetrachlorobenzoquinone (TCBQ)-caused toxicities in neuron-like cells which implies its association with neurodegenerative disorders. Although it is known that TCBQ induces oxidative damage, in turn results in endoplasmic reticulum (ER) stress and apoptosis, however, it is unclear how TCBQ trigger the signaling switch from pro-survival (to restore cellular homeostasis) to pro-death (trigger apoptosis). Protein disulfide isomerase family proteins (PDIs) regulate the progress of various neurodegenerative disorders, including Parkinson's disease and Alzheimer's disease. We tested the hypothesis that subcellular translocation of PDIs implicates survival/death signaling switch by inducing mitochondrial outer membrane permeabilization (MOMP). The rat pheochromocytoma PC12 cells were exposed to TCBQ and the concentration-dependent ER stress was observed upon TCBQ treatment, as indicated by increase in inositol-requiring kinase/endonuclease 1α (IRE1α) phosphorylation, C/EBP homologous protein (CHOP) expression, X-box-binding protein 1 (XBP1) splicing and caspase 12 activation. Interestingly, pharmacological (or siRNA) abrogation of PDIA1/PDIA3 aggravated loss of cell viability induced by relatively low concentration (10 μM) of TCBQ. However, inhibition of PDIA1/PDIA3 rescued high concentration (20 μM) of TCBQ-induced cell death. Further mechanistic study illustrated that PDIs initially acted to restore cellular homeostasis to pro-survival, but constant ER stress promoted signaling switch to pro-apoptotic by the release of PDIA1/PDIA3 from ER lumen to induce Bak-dependent MOMP. Our findings suggested that subcellular translocation of PDIs determined the "live or death" fate of PC12 cells to TCBQ-induced oxidative insult.

Keywords: Tetrachlorobenzoquinone; Protein Disulfide Isomerase; Endoplasmic Reticulum Stress; Apoptosis; Reactive oxygen species; Bak

INTRODUCTION

Neurodegenerative disorders are a group of neurological diseases and their pathogenesis are complicated. Most of them are characterized by the accumulation of misfolded proteins in neurons, leading to endoplasmic reticulum (ER) stress and cell dysfunction. Unfolded protein response (UPR) is triggered by ER stress when there is an imbalance between the folding capacity of ER and protein synthesis.[1] The UPR acts to re-establish homeostasis by a sophisticated transcription and translation signaling network to pro-survival, but constant ER stress promotes signaling switch from pro-survival to pro-apoptosis.[2]

ER stress-induced apoptosis may be caused by multiple environmental and pathological factors, but the precise mechanisms need to be further investigated. The protein disulfide isomerase family proteins (PDIs) regulate the progress of various neurodegenerative disorders, including Parkinson's disease, Alzheimer's disease and prion disorders.[3] PDIs play a crucial role in promoting of the folding of proteins and catalyzing the formation of disulfide bonds. Increasing evidence suggests that several endogenous ER luminal chaperones, released from the ER lumen have a unique pro-apoptotic activity in a variety of apoptotic events.[4, 5] Study has shown that abnormal distribution of PDIs on ER-mitochondrial junction results in neurotoxicity in Huntington and Alzheimer's disease models, and this effect is specific for misfolded proteins.[6]

TCBQ is a reactive metabolite of hexachlorobenzene (HCB) and pentachlorophenol (PCP), which have been widely used as pesticides. Because of their stable chemical properties, HCB and PCP remain threatening to human health. HCB can be found in the environment, blood, breast milk or adipose tissue of human.[7, 8] PCP, a major metabolite of HCB, was also detected in the urine, blood and adipose tissue of people.[9] They participate in a variety of biological and chemical processes,

including microorganism metabolism, post-translational modification of proteins and regulation of cellular signaling. HCB can easily cross the blood-brain barrier and accumulate in the brain, so it is considered as a potential neurotoxicant.[10] In addition, previous studies have also illustrated the neurotoxic behavior of PCP.[11, 12] TCBQ is the most toxic in a series of quinones,[13] which has better capacity of neurotoxicity than HCB and PCP.[14] More than 20% of PCP can be metabolized to TCHQ and TCBQ.[15] In addition, TCBQ was also widely used as a fungicide. TCBQ analogs have been identified as byproducts of drinking water disinfection.[16]

Our work recently highlighted that TCBQ perturbs the ER lumen of PC12 cells in a reactive oxygen species (ROS)-dependent mechanism.[17] The apoptosis of PC12 cells induced by TCBQ is associated with a sustained ER stress, up-regulating death receptor (DR) 5 (DR5) expression and enhancing the formation of death-inducing signaling complex (DISC). These results indicated the combination of ER stress and DR signaling pathways in TCBQ-induced neurotoxicity.

Given the broad importance of PDIs in regulation of cellular responses to various neurodegenerative disorders, the aim of this work was to investigate whether PDIs were involved in ER stress-induced apoptosis in TCBQ-treated PC12 cells, as well as the mechanisms leading to pro-apoptotic signaling. Our findings suggested that TCBQ promoted the role of PDIs switch from pro-survival to pro-apoptotic by the release of PDIA1 and PDIA3 from ER lumen into cytosol, then, induce Bak-dependent MOMP.

MATERIALS AND METHODS

Materials and Reagents

TCBQ was obtained from Aladdin Reagent Database Inc. (Shanghai, China). Methylmethane thiosulphonate (MMTS), 4-phenylbutyrate (4-PBA) and N-acetyl-l-cysteine (NAC) were supplied by Sigma-Aldrich Inc. (St. Louis, MO, USA). Bacitracin was purchased from Selleckchem (USA). Securinine was obtained from Yuanye Bio-Technology Co., Ltd. (Shanghai, China). Lactate dehydrogenase (LDH) assay kit was obtained from Nanjing Jiancheng Bioengineering Institute (Nanjing, China). Fura-2/AM, mitochondrial membrane potential assay kit with JC-1, BeyoECL Star and 6-Diamidino-2-phenylindole dihydrochloride (DAPI) were supplied by Beyotime Institute of Biotechnology (Nanjing, China). Cell counting kit-8 (CCK-8) was purchased from Genview (Shanghai, China). Bis(maleimido)hexane was obtained from TCI Development Co., Ltd. (Shanghai, China). S-Nitroso-L-glutathione (GSNO) was purchased from Cayman Chemical Company (USA). PDIA1 antibody, Smac antibody and Thiomuscimol were supplied by Santa Cruz Biotechnology (Santa Cruz, CA). Antibodies against KDEL, inositol-requiring kinase/endonuclease 1α (IRE1α), p-IRE1α (Ser726) and p-c-Jun N-terminal kinase (JNK) (Thr183) were purchased from Biosynthesis Biotechnology Co. Ltd. (Beijing, China). Antibodies against PDIA3, cytochrome *c*, calnexin, JNK, cyclooxygenase (COX) IV, c-Jun, ATF6 and caspase 12 were supplied by Proteintech group, Inc. (Wuhan, China). Avidin Resin and β-actin antibody were obtained from Sangon Biotech Co., Ltd. (Shanghai, China). Bak and Bax antibodies were supplied by Wanleibio Co., Ltd. (Shenyang, China). All other chemicals used were of the highest commercial grade.

Cell Culture and Treatment

The rat pheochromocytoma PC12 cell line was purchased from Nanjing Keygen Biotech. Co., Ltd. (Nanjing, China). Cells were cultured in growth media [Dulbecco's modified eagle's medium (DMEM), supplemented with 10% heat-inactivated newborn calf serum, 100 μg/mL streptomycin

and 100 U/mL penicillin] and incubated at 37°C with 5% CO_2 humidified atmosphere. Differentiation was carried out 24 hr after the cells were seeded by adding 50 ng/mL nerve growth factor (NGF) for 8 days. Then cells were harvested and were exposed to different concentrations of TCBQ for 24 hr. Control cells were cultured with equal amount of DMSO (always <0.1% in the culture). For the protection assay, cells were pretreated with 5 mM NAC or 5 mM 4-PBA for 1 hr, then exposed to 20 μM TCBQ for 24 hr.

CCK-8 and LDH Activity Assay

Cell viability was determined by CCK-8 assay (Bimake, USA). Briefly, cells were seeded in 96-well plates at a density of 5×10^3/well. After attached on the plates, cells were pretreated with PDI inhibitors or transfected with PDI siRNA, respectively, then incubated with different concentrations of TCBQ for 24 hr. Subsequently, the medium was replaced with 90 μL of fresh DMEM and 10 μL of kit reagent followed by 2~4 hr incubation. The absorbance of solution was measured at 450 nm using a microplate reader (BioTek ELX800).

The LDH assay, a test to evaluate cell integrity was performed using a commercial kit according to the manufacturer's protocol. At the end of incubation, cell medium was centrifuged, and the supernatant was collected. The amount of LDH released in the supernatant was assayed following the manufacturer's instructions. All experiments were carried out in triplicate.

Small RNA (siRNA) Interference

PC12 cells were transfected with control scrambled siRNA or indicated siRNA using siRNA-mate transfection reagent (Shanghai GenePharma Co. Ltd.) according to the manufacturer's protocol. Following a 48 hr knockdown, cells were stimulated with TCBQ for 24 hr. The sequences

for each pair of siRNA were listed in **Table 1** and prepared according to the manufacture's recommendation.

Protein Extraction and Western Blotting

Proteins were prepared with RIPA lysis buffer [150 mM NaCl, 50 mM Tris-HCl (pH 7.4), 1% NP-40, 0.1% SDS, 0.5% sodium deoxycholate, 1 mM PMSF and proteinase inhibitor cocktail]. The total protein concentration was determined with a BCA assay kit (Dingguo Biotechnology Co., Ltd. Beijing, China). Protein was separated by SDS-polyacrylamide gel electrophoresis (SDS-PAGE) and transferred onto a nitrocellulose membrane. Membranes were blocked with 5% BSA and then incubated overnight with appropriate primary antibodies at 4°C. After washing in TBST three times, the membranes were further incubated with the secondary antibody for additional 1 hr at room temperature. The signals were detected using BeyoECL Star (Beyotime Biotechnology, Shanghai, China). Representative blots were chosen from at least three independent experiments and the expression levels of proteins were performed by ImageJ software (National Institutes of Health, Maryland, USA). β-Actin was used as a housekeeping gene in the experiments.

Biotin-Switch Assay for SNO-PDIs

Detection of PDIs S-nitrosylation with biotin-switch technique was performed as described previously.[18] Briefly, cells were lysed as desired in HENT buffer [250 mM HEPES (pH 7.4), 1 mM EDTA, 0.1 mM neocuproine and 1% Triton X-100]. For experiments employing 2 mg of total protein, blocking buffer (final concentration with 2.5% SDS and 0.1% MMTS in HEN buffer) was mixed with the samples and incubated at 50°C in the dark for 20 min with frequent vortexing to block free thiol groups. After MMTS was removed by acetone precipitation, HENS buffer (HEN buffer with 1% SDS) containing sulfhydryl-specific biotinylated reagent biotin-HPDP (0.25 mg/mL)

and 20 mM sodium ascorbate was added to each sample. Samples were rotated in the dark for 1 hr at room temperature. Nitrosothiols were reduced to thiols and then linked to biotin-HPDP in this step. The excess biotin-HPDP was removed by acetone precipitation. The biotinylated proteins were pulled down using prewashed avidin-affinity resin. After eluted with elution buffer containing 1% β-mercaptoethanol, the supernatant was collected without disturbing the pelleted resin and subjected to Western blotting to determine the amount of PDIs remaining in the samples. Note that in this experiment, cell lysate was divided into two parts. One half was to evaluate SNO-PDIs formation using a biotin-switch assay, the other half was used to detect the total amount of PDIs.

Subcellular Fractionation

Cytosolic, mitochondrial, and ER-microsomal cell fractions were isolated from PC12 cells as described previously with some modification.[19] In brief, 5×10^7 cells were collected by centrifugation at 600 g for 5 min and washed by re-suspending cells with PBS. Then, cells were resuspended with homogenizing buffer [10 mM HEPES (pH 7.5), 250 mM sucrose, 25 mM KCl, 1 mM EDTA and a proteinase inhibitor cocktail] plus homogenized 30-50 passes with ice-cold dounce tissue homogenizer. The homogenates were transferred to a 1.5 mL microcentrifuge tube and centrifuge at 1,000 g for 10 min. The post-nuclear supernatants were centrifuged at 10,000 g for 10 min at 4°C to pellet mitochondria. The post-mitochondrial supernatants were centrifuged at 100,000 g for 60 min at 4°C to pellet ER-microsomal. The supernatants were transferred to clean tubes to obtain cytosolic fraction. The mitochondrial and ER-microsomal pellets were lysed in 1% ice-cold Triton lysis buffer [50 mM Tris-HCl (pH 7.5), 150 mM NaCl, 1% Triton, 1 mM EDTA, 1 mM EGTA and proteinase inhibitor cocktail] for 20 min and then sonicated three times for 20 s. The lysates were centrifuged at 12,000 g for 10 min, then supernatants were collected and used for Western blotting.

Immunofluorescence Double Staining

PC12 cells were plated onto confocal dishes overnight for adherence. Then, cells were exposed to 20 μM TCBQ for 24 hr followed by fixed in 4% paraformaldehyde for 30 min, permeabilized with 1% Triton X-100 for 10 min and blocked with 10% BSA at 4°C for 1 hr. Cells were incubated with mouse anti-PDIA1 and rabbit anti-calnexin for 2 hr, respectively, followed by incubation with goat anti-mouse (Alexa Fluor 488) and goat anti-rabbit secondary antibodies (Cy3) for an additional 1 hr. Finally, the pictures were taken by fluorescent microscopy (OLYMPUS IX71).

Measurement of Mitochondrial Membrane Potential (MMP)

The loss of MMP was an evidence of decreased cell viability. Detection of MMP using JC-1 probe was performed as described previously.[20] At low MMP, JC-1 accumulated in cytosol as monomers and emitted green fluorescence. At high MMP, JC-1 preferentially gone into mitochondria and aggregated, then its fluorescence turned to red. After exposed to TCBQ, PC12 cells were treated with JC-1 at a concentration of 1 μg/mL for 20 min and washed with PBS. Images were visualized by fluorescent microscope (OLYMPUS IX71).

Real-time quantitative PCR (RT-PCR) and RT-qPCR

Total RNA was isolated by RNA Purification Kit (BioTeke, BeiJing, China) according to the recommended protocol. The purified RNA (2 μg) was reverse transcribed into cDNA using All-in-One cDNA Synthesis SuperMix (Bimake, USA). For detecting the splicing of X-box-binding protein 1 (XBP1), cDNA was then amplified by RT-PCR using 2× Taq plus PCR Master Mix (DBI Bioscience, Germany). The primers could specifically amplify both spliced and un-spliced rat XBP-1 isoforms. PCR was initiated at 94°C for 3 min, 30 cycles of 94°C for 30 s, 55°C for 30 s, and 72°C for 1 min, followed by a final incubation at 72°C for 5 min. The amplified products were separated

using 7.5% SDS-PAGE. The DNA was stained with ethidium bromide and visualized under UV light.

Quantitative analysis of mRNA expression was performed *via* RT-qPCR using 2× SYBR Green qPCR Master Mix (Bimake, USA) and BioRad CFX96™ Real Time System. Gene-specific primers were listed in **Table 2**. The cycling conditions consisted of initial denaturing at 95°C for 10 min, 40 cycles of denaturation at 95°C for 10 s, annealing at the most suitable temperature for 30 s, and extension at 72°C for 30 s, followed by a final incubation at 72°C for 10 min. Data from three independent experiments were analyzed and relative gene expression normalized to housekeeping gene β-actin was calculated using the $2^{-\Delta\Delta Ct}$ method.[21]

Cytosolic Ca^{2+} Measurement

Cytosolic Ca^{2+} was examined as described previously with minor modification.[22] Briefly, PC12 cells were collected and adjusted to a density of 2×10^6 cells/mL, then incubated with 4 μM Fura-2/AM for 1 hr at 37°C in Krebs–Ringer bicarbonate buffer (KRB-HEPES) [119 mM NaCl, 1.0 mM $CaCl_2$, 4.8 mM KCl, 1.2 mM KH_2PO_4, 1.2 mM $MgSO_4$, 25 mM $NaHCO_3$, 10 mM HEPES (pH 7.5) and 5.5 mM glucose]. After loading, cells were washed three times followed by remaining suspended in KRB-HEPES. The fluorescence intensities were recorded in the ratio mode at 340 and 380 nm excitation wavelength and 510 nm emission wavelength with a fluorescence spectrophotometer (Hitachi, Japan). Cells were continuously stirred throughout the experiment. The corresponding ratio (F340/F380) was used to obtain intracellular concentrations of free Ca^{2+}, $[Ca^{2+}]_i$, by using following equation: $[Ca^{2+}]_i = K_d\times(R-R_{min})/(R_{max}-F)(S1/S2)$ (nmol/L). R_{min}-ratio at zero free Ca^{2+}, R_{max}-ratio at saturating Ca^{2+}, K_d was 224 nM at 37°C. All experiments were carried out in triplicate.

Detecting Bak and Bax Oligomerization on Mitochondria

Mitochondria were isolated from PC12 cells by Cytoplasmic and Mitochondrial Protein Extraction Kit (Sangon Biotech Co., China) according to the recommended protocol. Cross-linking experiment was performed as described previously with some modification.[23] Mitochondrial pellets were incubated with the cross-linking agent bis(maleimido)hexane (0.1 mM) in MIB buffer [300 mM sucrose, 0.1% BSA, 10 mM HEPES (pH 7.5), 1.5 mM $MgCl_2$, 10 mM KCl, 1 mM EDTA, 1 mM EGTA] at 25°C for 1 hr. Then, mitochondria were washed in MIB buffer and dissolved in 1× SDS-PAGE loading buffer for Western blotting.

Terminal Transferase-mediated dUTP-biotin Nick End Labeling (TUNEL) Assay

DNA fragmentation was detected by TUNEL kit (Beyotime Institute of Biotechnology, Nanjing, China). Cells were washed in PBS for 5 min, and fixed in 4% paraformaldehyde for 10 min. TUNEL assay was performed according to manufacturer's instruction. Fluorescent signal was analyzed by a fluorescent microscope. The apoptotic cells were detected by immunofluorescent staining with TUNEL (red). DAPI (blue) staining was used to label the nuclei.

Statistical Analysis

Data were generated by at least three independent experiments and expressed as mean ± SD. SPSS 19.0 software was used to analyze significant differences using a one-way ANOVA followed by least significance difference (LSD) multiple comparison tests. A value of p less than 0.05 was considered to be statistically significant.

RESULTS

TCBQ Exposure Induces ER Stress in PC12 Cells

We adapted PC12 cell line, a well-established *in vitro* experimental model to detect the neurotoxic potential of TCBQ.[17] To determine whether ER stress was induced upon TCBQ treatment, we examined the activation status of three branches in UPR signaling pathways. The phosphorylated form of IRE1α was significantly increased in PC12 cells exposed to TCBQ in a concentration (**Figure 1A**) and time-dependent manner (**Figure S1A**). Upon ER stress, the activation of IRE1α promoted the phosphorylation of JNK[24] or initiated the splicing of XBP-1 mRNA to its spliced variant XBP-1s.[25] TCBQ treatment showed no effects in the activation of JNK and the downstream expression of c-Jun (**Figure 1A** and **Figure S1A**). Given the important roles of XBP-1 in signaling pathways induced by ER stress, we next examined the effect of TCBQ on the level of XBP-1s mRNA using RT-PCR. TCBQ stimuli resulted in a dose and time-dependent up-regulation of spliced XBP-1s (**Figure 1B** and **Figure S1B**). Subsequent RT-qPCR analyses also showed enforced expression of XBP-1s mRNA by TCBQ treatment. Our result showed that TCBQ-induced ER stress was JNK-independent but XBP-1-dependent. ER stress may result in an active short form of ATF6, which activates the promoters of ER chaperone genes.[26] However, neither precursor nor the cleavage of ATF6 was significantly altered (**Figure 1C** and **Figure S2A**). Our previous studies have shown that TCBQ could activate PERK-ATF4-CHOP signaling pathway in protein levels.[17] Consistently, the increase in ATF4 and CHOP mRNA expression were occurred in the presence of TCBQ (**Figure 1D**, **1E**, **Figure S2B** and **S2C**). ER is one of the intracellular Ca^{2+} pools and plays an important role in Ca^{2+} homeostasis.[27] Therefore, we also studied the effect of TCBQ on intracellular Ca^{2+} homeostasis. The effect of TCBQ on cytosolic free calcium concentration ($[Ca^{2+}]_i$) was measured by the Fura-2/AM fluorescent probe in PC12 cells. The increase of $[Ca^{2+}]_i$ began at 5 μM TCBQ and peaked at 15 μM TCBQ (**Figure 1F**). Caspase 12 is the first caspase reported to localize on the ER,

which can be activated when intracellular Ca^{2+} imbalance or accumulation of excessive misfolding protein in the ER.[28] Consistent with the increase of $[Ca^{2+}]_i$, we found that TCBQ treatment activated caspase 12, as indicated by an increased tendency of cleaved caspase 12 (**Figure 1G** and **Figure S2D**). Furthermore, we compared the effects of HCB, PCP, TCHQ and TCBQ on ER stress in PC12 cells. Up to 20 μM and 24 hr exposure, HCB and PCP were substantially ineffective for ER stress. TCHQ and TCBQ had the similar ability to activate ER stress, such as the activation of GRP78, p-PERK, ATF4, p-IRE1α and caspase 12 (**Figure S3**). These results indicated that TCBQ has a better capacity than its precursors HCB and PCP on ER stress. To sum up, TCBQ exposure showed an increase in IRE1α phosphorylation, CHOP expression, XBP1 splicing and caspase 12 activation.

Dual function of PDIs on TCBQ-induced cytotoxicity

The UPR acts to restore cellular homeostasis to pro-survival, but constant or severe ER stress promotes signaling switch from pro-survival to pro-apoptotic.[29] We have demonstrated that TCBQ utilizes ER stress-induced apoptosis by DR5 expression,[17] the precise mechanism needs to be further investigated. Moreover, several PDI members involve in multiple phases of ER stress, which initial response is pro-survival through its molecular chaperones and isomerase activity,[30, 31] while subsequent effect is pro-apoptotic when repair has been considered invalid.[32] Here, we explored the role of PDIs in ER stress-induced apoptosis under TCBQ treatment. PC12 cells were treated with 10 μM or 20 μM TCBQ in the absence or presence of PDI inhibitors,[23] cell viabilities were examined at 24 hr post-induction and plotted as a percentage for the comparison with untreated group. As shown in **Figure 2A-2C**, within 10 μM TCBQ group, securinine, thiomuscimol and bacitracin provided a dose-dependent aggravation of TCBQ-induced cytotoxicity, suggested the pro-survival role of PDI.

Whereas in the case of 20 μM TCBQ group, these three inhibitors alleviated TCBQ-induced loss of cell viability, implicated the pro-death effect of PDI.

Furthermore, we examined the role of PDIs in TCBQ-induced cytotoxicity by PDIA1 and PDIA3 siRNA. PC12 cells were transfected with three different siRNA in indicated concentrations, respectively, to achieve diverse sub-saturating levels of PDI proteins silencing. Consistently, when PDIA1 was knockdown by siRNA, we observed a aggravated loss of cell viability with 10 μM TCBQ treatment and a alleviated loss of cell viability with 20 μM TCBQ treatment (**Figure 2D**). Differences in the results of some siRNA groups may be related to their interference efficiency, since excessive inhibition of PDI was toxic. However, the decreased expression of PDIA3 was associated with the elevation of cell viability in most of the groups (**Figure 2E**). We found PDIA3 has a higher pro-apoptotic potency in PC12 cells, as indicated by the rescue of PDIA3 siRNA at 10 μM TCBQ exposure. These data suggested that both PDIA1 and PDIA3 were involved in the neurotoxicity of TCBQ in PC12 cells, analogously to p53 expression, which initiates to repair damaged DNA but induces cell apoptosis at extreme thresholds of DNA damage.[33, 34] These results indicated that the protective or harmful functions of PDI proteins may be modulated by the level of ER stress.

TCBQ Shows No Effect on the Expression or S-nitrosylation of PDIs

We further quest the mechanism of PDIs as a pleiotropic apoptotic regulator under TCBQ treatment. It was speculated that protein expression and post-translational modification of susceptible thiols may determine the protective or apoptotic role of PDIs. To monitor PDIs protein expression, cells were treated with TCBQ for 24 hr. Dose-response (**Figure 3A** and **3B**) and time-course (**Figure S5A** and **S5B**) experiments showed that PDIA1 and PDIA3 expressions have no significant change in PC12 cells.

To further explore the post-translational modification of PDI, we measured S-nitrosylated PDIA1 (SNO-PDIA1), which was formed by adding NO to active site cysteine residues and implicated in several neurodegenerative diseases.[35] After treatment with TCBQ, SNO-PDIA1 did not occur in PC12 cells, as detected by biotin-switch assay, indicating that S-nitrosylation of PDIA1 was not triggered by TCBQ stimuli (**Figure 3C**). TCBQ is a potent alkylating agent that has strong affinity towards thiols.[36] Thus, covalent modification of thiol groups in PDIs by TCBQ might occur in cells. If Cys thiols site of TCBQ binding was consistent with the site of S-nitrosylation, then S-nitrosylation level of PDIA1 should be reduced significantly under TCBQ treatment. To rule out this hypothesis, PC12 cells were pre-incubated with different concentrations of TCBQ for 24 hr and then treatment with (or without) 100 μM GSNO for 30 min. No decrease in SNO-PDIA1 level was observed with TCBQ treatment (**Figure 3D**). These results suggested that TCBQ may not influence the protein expression and S-nitrosylation modification of PDIs in PC12 cells.

TCBQ Triggers Cytosolic Translocation of PDIs and Induces MOMP

Previous study has indicated that the protective or pro-apoptotic role of PDIs may be related to its subcellular localization.[3] To better understand how PDIs regulate TCBQ's neurotoxicity, we examined the localization of PDIA1 and PDIA3 in subcellular fractions of induced PC12 cells. After TCBQ exposure, PC12 cells dramatically accumulated PDIs (PDIA1 and PDIA3) in cytosol fractions in a dose-dependent manner (**Figure 4A**). PDIs in the mitochondrial fractions were slightly up-regulated (significant difference only found in 20 μM group, $p<0.01$). Consistent down-regulation of PDIs in ER-microsomal fractions were found (~50% of loss compared with the control in 20 μM group). This phenomenon suggested that the release of PDIs from ER lumen to cytosol upon TCBQ treatment. Interestingly, the level of PDIA3 in cytosol/ER fractions of cells under TCBQ stimuli was

higher than that of PDIA1 (**Figure 4A**), indicating PDIA3 was more sensitive to TCBQ-induced leak of ER luminal proteins and then function to promote apoptosis. This explained that the knockdown of PDIA3 enhanced cell survival at 10 μM TCBQ treatment, while the knockdown of PDIA1 exhibited pro-apoptotic character. In agreement with the results of Western blotting, immunofluorescent double staining result showed PDIA1 was primarily co-localized with calnexin in resting PC12 cells, but 20 μM TCBQ caused the partially dislocation of PDIA1 with calnexin, which was a marker of ER (**Figure 4B**). To study how the subcellular localization of PDIs on the regulation of apoptosis, we examined the effect of PDIs on MOMP. Cytochrome *c* release, which was determined as a parameter of MOMP, was greatly stimulated by TCBQ in a dose-dependent manner (**Figure 4C**), and knockdown of PDIs in PC12 cells suppressed the release of cytochrome *c* and smac (**Figure 4D**). MOMP often leads to the loss of MMP. With 20 μM TCBQ treatment, cells showed a significant reduction of red fluorescence (JC-1 aggregates) intensity along with an increase of green fluorescence (JC-1 monomer), indicating the compromised outer mitochondrial membrane integrity could be rescued by blocking the catalytic activity of PDIs with small-molecule inhibitors (**Figure 4E**) or silencing expression of PDIA1 (**Figure S6**). Taken together, these evidences indicated that TCBQ induced PDIs accumulation in cytosol, then induced MOMP.

PDIs Play an Important Role in TCBQ-mediated Bak Oligomerization in Mitochondria, Which Contribute to MOMP

The release of cytochrome *c* is mediated by Bcl-2 protein family, which localize on the mitochondria. MOMP is primarily inducted by homo-oligomeric channels of Bak or Bax in mitochondrial outer membrane.[37] The pore-forming capability of Bax or Bak oligomers leads to the permeabilization of mitochondrial outer membrane and then the release of cytochrome *c* into cytosol.

To better understand how PDIs manipulate TCBQ-induced apoptosis, we examined PDI-induced oligomerization of Bcl-2 protein family with 20 μM TCBQ treatment, in which concentration a significant cytosol localization of PDIs was found. After incubation with TCBQ for 24 hr, the mitochondria fraction was isolated and the cross-linking experiment for detection of oligomeric proteins was performed as described in "Materials and Methods." TCBQ induced the formation of Bak dimer and trimer on mitochondria in a PDIs-dependent manner. The knockdown of PDIA1 or PDIA3 in TCBQ-induced PC12 cells could antagonize TCBQ-induced oligomerization of Bak, suggesting Bak functions as a downstream effector of PDIs (**Figure 5A**). However, TCBQ did not affect the oligomerization of Bax (**Figure 5B**). Although the underlying molecular mechanism how TCBQ-mediated Bak assembly was unclear, previous study confirmed that Bax can form an active oligomeric complex by oxidizing its cysteine residue[38]. Since TCBQ has a potential on the conjugation of cysteine thiol,[39] this mechanism may also apply to the current study. These results showed Bak oligomerization occurred simultaneously with the increase in TCBQ-mediated MOMP, suggesting that PDIA1 and PDIA3 may be involved in TCBQ-mediated MOMP by triggering of Bak, but not Bax, oligomerization in mitochondria and subsequent mitochondrial dysfunction in PC12 cells.

ROS Generation Plays an essential role on PDIs Translocation and Pro-death

Certain luminal chaperones released from ER lumen may involve in the ER stress-induced apoptosis in various apoptotic events.[4, 40] We have demonstrated that TCBQ-induced ER stress is mediated by ROS. Thus, NAC and 4-PBA were employed in this study as the inhibitors of ROS and ER stress, respectively. Western blotting analysis revealed that NAC and 4-PBA both prevented TCBQ-induced increase of PDIs in cytosol fractions, indicating that TCBQ induced ER stress

through ROS stimuli and then leaded the leakage of PDIs from the ER to cytosol (**Figure 6A**). The blockage of ROS with NAC inhibited TCBQ-induced TUNEL-positive cells (**Figure 6B**), alleviated the decrease of cell viability (**Figure 6C**) and attenuated the increasing of intracellular LDH (**Figure 6D**). These results suggested that ROS formation was an initial step of TCBQ-induced PDIs release from ER stress and consequent apoptosis.

DISCUSSION

Neurodegenerative diseases are a large class of neurological diseases and also known as protein misfolding diseases associated with the misfolded protein accumulation of plaques.[41] The pathogenesis of neurodegenerative diseases are complex, including gene mutations, epigenetic changes, oxidative stress, metabolism disorder, abnormal protein modification and deposition.[42] However, environmental pollutants have not been listed as a risk factor for neurodegenerative diseases. At present, HCB and PCP can still be detected in the environment and human body, and their toxicity have also been widely recognized.[7, 9] It has been confirmed that the cytotoxicity of TCBQ is greater than its precursors HCB and PCP,[14] which is consistent with our finding that TCBQ has better capacities than its precursors HCB and PCP on the introducing of ER stress. Therefore, the determination of TCBQ-caused neurotoxicity may help to understand the exact toxic mechanism of its precursors.

Oxidative stress, as a result of the imbalance between oxidants and antioxidants, results in the accumulation of ER stress.[43] Arylating quinone-induced toxicity may involve Michael adduct formation and also results in ER stress.[44] As a full substituted halogenated quinone, TCBQ may conjugate with thiol group on the proteins *via* “chlorine displacement” reaction.[36] Thus,

TCBQ-induced ER stress may have two different mechanism, *i.e.*, oxidative stress and arylation with nucleophiles (cysteinyl thiols on the proteins). Previous finding suggested that ROS is upstream of the UPR, thus, antioxidants can reduce UPR signaling.[45, 46] This statement is also further confirmed by the current study by inhibiting ROS propagation with NAC. Moreover, proteomics examination demonstrated that PDIs act as the targets of quinones.[47] Whether TCBQ direct modify thiol groups on PDIs and the biological consequences need further investigation.

In response to oxidative stress-mediated aberrant protein folding and accumulation, ER stress often results in chaperone up-regulation, particularly PDI family proteins, served as a vital cellular defense against aberrant proteins.[48] The putative redox effect of PDIs and its possible functional role in disease have been recently reviewed .[49] In the present study, we investigated the role of PDIA1 and PDIA3 in TCBQ-induced apoptosis. We demonstrated that inhibitors or siRNA of PDIs provided a promotion of apoptosis under 10 μM TCBQ treatment and a rescue of TCBQ toxicity under 20 μM TCBQ treatment in PC12 cells, suggesting the pro-survival role of PDIs at the early stage of ER stress condition, but constant ER stress promoted signaling switch to pro-apoptotic. Hoffstrom *et al* reported that the inhibition of PDIs suppress apoptotic signaling induced by misfolded proteins, which also supported that PDIs play an important role on quality control in protein folding and show pro-apoptotic function.[6] Of note, although previous studies demonstrated that sustained ER stress promotes the increased expression of PDI at the protein and mRNA levels,[46, 50] PDIs expressions have not been affected by TCBQ. The function of PDIs may be abolished due to abnormal post-translational modifications.[35] S-nitrosylation is the most studied form of modification, which involved in the inhibition of chaperone/isomerase activities of PDIs.[35, 51, 52] Unexpectedly, we observed that the conversion of PDIs function unrelated with its expression nor SNO modification.

Although PDIs are mainly located in ER lumen, they can be translocated into other compartments of the cells, *e.g.*, mitochondria, nucleus and cytosol.[49] However, it is current unclear how the location of PDI affects its canonical ER functions.[53] PDIs transfer to the ER-mitochondrial junction result in MOMP [6], which is in parallel with the current study that TCBQ promoted signaling switch to pro-apoptotic by the release of PDIA1 and PDIA3 from ER lumen to induce Bak-dependent MOMP. Not just translocated into other compartments of the cells, PDIs have also been detected at the cell surface (position itself into membranes), the mechanisms and implications have been reviewed.[49, 54]

Increasing evidences suggested the connection of PDI function with its mitochondria subcellular location. The proper maintenance of the mitochondrial is crucial for the quality control of cells and ER-mediated UPR largely contributed to resist ROS insults. [55] The expressions of mitochondrial-protective Lon protease transmit oxidative stress from ER to mitochondria.[56] More significantly, under severe conditions, ER stress-induced IRE1α signaling is activated through direct interaction of BH1 and BH3 domains of BAK with IRE1α, which provided a direct link between the apoptotic pathway and UPR.[57] Among the UPR to pro-apoptotic signaling pathways, BAK oligomerization is essential for the full activation of IRE1α.[6, 57] Interestingly, PDIs control the duration of IRE1α activity and thus limit UPR signaling.[58] Together, these findings indicated the dual pro- and anti-apoptotic function of PDIs,[3] which both reflected in TCBQ-induced neurotoxicity.

CONCLUSION

Our results showed that the implicating neurotoxicity of TCBQ was related to its effects on PDIs biological functions. This finding not only clarifies the mechanism of TCBQ neurotoxicity, but also indicates that PDI proteins can be used as targets for antagonizing TCBQ toxicity.

SUPPORTING INFORMATION AVAILABLE

Experimental details, Figures S1−S6 (PDF). This material is available free of charge via the Internet at http://pubs.acs.org.

AUTHOR INFORMATION

Funding

This work is supported by National Natural Science Foundation of China (21622704, 21575118 and 21477098)

Notes

The authors declare no competing financial interest.

Abbreviations

CCK-8, cell counting kit-8; CHOP, C/EBP homologous protein; COX, cyclooxygenase; DAPI, 6-Diamidino-2-phenylindole dihydrochloride; DISC, death-inducing signaling complex; DMEM, Dulbecco's modified eagle's medium; DR, death receptor; ER, endoplasmic reticulum; GSNO, S-nitroso-L-glutathione; HCB, hexachlorobenzene; IRE1α, inositol-requiring kinase/endonuclease

1α; JNK, c-Jun N-terminal kinase; LDH, lactate dehydrogenase; MMP, mitochondrial membrane potential; MMTS, methylmethane thiosulphonate; MOMP, mitochondrial outer membrane permeabilization; NAC, N-acetyl-l-cysteine; 4-PBA, 4-phenylbutyrate; PCP, pentachlorophenol; PDIs, protein disulfide isomerase family proteins; ROS, reactive oxygen species; RT-qPCR, real-time quantitative PCR; SDS-PAGE, SDS-polyacrylamide gel electrophoresis; TCBQ, tetrachlorobenzoquinone; TUNEL, terminal transferase-mediated dUTP-biotin nick end labeling; UPR, unfolded protein response; XBP1, X-box-binding protein 1

REFERENCES

(1) Lin, J. H., Walter, P., and Yen, T. S. (2008) Endoplasmic reticulum stress in disease pathogenesis. *Annu Rev Pathol 3*, 399-425.

(2) Rasheva, V. I., and Domingos, P. M. (2009) Cellular responses to endoplasmic reticulum stress and apoptosis. *Apoptosis 14*, 996-1007.

(3) Grek, C., and Townsend, D. M. (2014) Protein Disulfide Isomerase Superfamily in Disease and the Regulation of Apoptosis. *Endoplasmic Reticulum Stress Dis 1*, 4-17.

(4) Burikhanov, R., Zhao, Y., Goswami, A., Qiu, S., Schwarze, S. R., and Rangnekar, V. M. (2009) The tumor suppressor Par-4 activates an extrinsic pathway for apoptosis. *Cell 138*, 377-388.

(5) Gardai, S. J., McPhillips, K. A., Frasch, S. C., Janssen, W. J., Starefeldt, A., Murphy-Ullrich, J. E., Bratton, D. L., Oldenborg, P. A., Michalak, M., and Henson, P. M. (2005) Cell-surface calreticulin initiates clearance of viable or apoptotic cells through trans-activation of LRP on the phagocyte. *Cell 123*, 321-334.

(6) Hoffstrom, B. G., Kaplan, A., Letso, R., Schmid, R. S., Turmel, G. J., Lo, D. C., and Stockwell, B. R. (2010) Inhibitors of protein disulfide isomerase suppress apoptosis induced by misfolded proteins. *Nat Chem Biol 6*, 900-906.

(7) Song, S., Ma, J., Tian, Q., Tong, L., and Guo, X. (2013) Hexachlorobenzene in human milk collected from Beijing, China. *Chemosphere 91*, 145-149.

(8) Ezendam, J., Staedtler, F., Pennings, J., Vandebriel, R. J., Pieters, R., Harleman, J. H., and Vos, J. G. (2004) Toxicogenomics of subchronic hexachlorobenzene exposure in Brown Norway rats. *Environ Health Perspect 112*, 782-791.

(9) Zheng, W., Wang, X., Yu, H., Tao, X., Zhou, Y., and Qu, W. (2011) Global trends and diversity in pentachlorophenol levels in the environment and in humans: a meta-analysis. *Environ Sci Technol 45*, 4668-4675.

(10) Escuder-Gilabert, L., Villanueva-Camanas, R. M., Sagrado, S., and Medina-Hernandez, M. J. (2009) Permeability and toxicological profile estimation of organochlorine compounds by biopartitioning micellar chromatography. *Biomed Chromatogr 23*, 382-389.

(11) Folch, J., Yeste-Velasco, M., Alvira, D., de la Torre, A. V., Bordas, M., Lopez, M., Sureda, F. X., Rimbau, V., Camins, A., and Pallas, M. (2009) Evaluation of pathways involved in pentachlorophenol-induced apoptosis in rat neurons. *Neurotoxicology 30*, 451-458.

(12) Tang, Y., Donnelly, K. C., Tiffany-Castiglioni, E., and Mumtaz, M. M. (2003) Neurotoxicity of polycyclic aromatic hydrocarbons and simple chemical mixtures. *J Toxicol Environ Health A 66*, 919-940.

(13) Siraki, A. G., Chan, T. S., and O'Brien, P. J. (2004) Application of quantitative structure-toxicity relationships for the comparison of the cytotoxicity of 14 p-benzoquinone congeners in primary cultured rat hepatocytes versus PC12 cells. *Toxicol Sci 81*, 148-159.

(14) Fu, J., Shi, Q., Song, X., Xia, X., Su, C., Liu, Z., Song, E., and Song, Y. (2016) Tetrachlorobenzoquinone exhibits neurotoxicity by inducing inflammatory responses through ROS-mediated IKK/IkappaB/NF-kappaB signaling. *Environ Toxicol Pharmacol 41*, 241-250.

(15) Reigner, B. G., Rigod, J. F., and Tozer, T. N. (1992) Disposition, bioavailability, and serum protein binding of pentachlorophenol in the B6C3F1 mouse. *Pharm Res 9*, 1053-1057.

(16) Zhao, Y., Qin, F., Boyd, J. M., Anichina, J., and Li, X. F. (2010) Characterization and determination of chloro- and bromo-benzoquinones as new chlorination disinfection byproducts in drinking water. *Anal Chem 82*, 4599-4605.

(17) Liu, Z., Shi, Q., Song, X., Wang, Y., Wang, Y., Song, E., and Song, Y. (2016) Activating Transcription Factor 4 (ATF4)-ATF3-C/EBP Homologous Protein (CHOP) Cascade Shows an Essential Role in the ER Stress-Induced Sensitization of Tetrachlorobenzoquinone-Challenged PC12 Cells to ROS-Mediated Apoptosis via Death Receptor 5 (DR5) Signaling. *Chem Res Toxicol 29*, 1510-1518.

(18) Forrester, M. T., Foster, M. W., Benhar, M., and Stamler, J. S. (2009) Detection of protein S-nitrosylation with the biotin-switch technique. *Free Radic Biol Med 46*, 119-126.

(19) Ye, Z. W., Zhang, J., Ancrum, T., Manevich, Y., Townsend, D. M., and Tew, K. D. (2017) Glutathione S-Transferase P-Mediated Protein S-Glutathionylation of Resident Endoplasmic Reticulum Proteins Influences Sensitivity to Drug-Induced Unfolded Protein Response. *Antioxid Redox Signal 26*, 247-261.

(20) Xu, D., Li, L., Liu, L., Dong, H., Deng, Q., Yang, X., Song, E., and Song, Y. (2015) Polychlorinated biphenyl quinone induces mitochondrial-mediated and caspase-dependent apoptosis in HepG2 cells. *Environ Toxicol 30*, 1063-1072.

(21) Livak, K. J., and Schmittgen, T. D. (2001) Analysis of relative gene expression data using real-time quantitative PCR and the 2(-Delta Delta C(T)) Method. *Methods 25*, 402-408.

(22) Nani, A., Belarbi, M., Ksouri-Megdiche, W., Abdoul-Azize, S., Benammar, C., Ghiringhelli, F., Hichami, A., and Khan, N. A. (2015) Effects of polyphenols and lipids from Pennisetum glaucum grains on T-cell activation: modulation of Ca(2+) and ERK1/ERK2 signaling. *BMC Complement Altern Med 15*, 426.

(23) Zhao, G., Lu, H., and Li, C. (2015) Proapoptotic activities of protein disulfide isomerase (PDI) and PDIA3 protein, a role of the Bcl-2 protein Bak. *J Biol Chem 290*, 8949-8963.

(24) Kaser, A., and Blumberg, R. S. (2009) Endoplasmic reticulum stress in the intestinal epithelium and inflammatory bowel disease. *Semin Immunol 21*, 156-163.

(25) Gardner, B. M., Pincus, D., Gotthardt, K., Gallagher, C. M., and Walter, P. (2013) Endoplasmic reticulum stress sensing in the unfolded protein response. *Cold Spring Harb Perspect Biol 5*, a013169.

(26) Ye, J., Rawson, R. B., Komuro, R., Chen, X., Dave, U. P., Prywes, R., Brown, M. S., and Goldstein, J. L. (2000) ER stress induces cleavage of membrane-bound ATF6 by the same proteases that process SREBPs. *Mol Cell 6*, 1355-1364.

(27) Hammadi, M., Oulidi, A., Gackiere, F., Katsogiannou, M., Slomianny, C., Roudbaraki, M., Dewailly, E., Delcourt, P., Lepage, G., Lotteau, S., Ducreux, S., Prevarskaya, N., and Van Coppenolle, F. (2013) Modulation of ER stress and apoptosis by endoplasmic reticulum calcium leak via translocon during unfolded protein response: involvement of GRP78. *FASEB J 27*, 1600-1609.

(28) Nakagawa, T., Zhu, H., Morishima, N., Li, E., Xu, J., Yankner, B. A., and Yuan, J. (2000) Caspase-12 mediates endoplasmic-reticulum-specific apoptosis and cytotoxicity by amyloid-beta. *Nature 403*, 98-103.

(29) Paschen, W., and Mengesdorf, T. (2005) Endoplasmic reticulum stress response and neurodegeneration. *Cell Calcium 38*, 409-415.

(30) Tanaka, S., Uehara, T., and Nomura, Y. (2000) Up-regulation of protein-disulfide isomerase in response to hypoxia/brain ischemia and its protective effect against apoptotic cell death. *J Biol Chem 275*, 10388-10393.

(31) Xu, D., Perez, R. E., Rezaiekhaligh, M. H., Bourdi, M., and Truog, W. E. (2009) Knockdown of ERp57 increases BiP/GRP78 induction and protects against hyperoxia and tunicamycin-induced apoptosis. *Am J Physiol Lung Cell Mol Physiol 297*, L44-51.

(32) Wang, S. B., Shi, Q., Xu, Y., Xie, W. L., Zhang, J., Tian, C., Guo, Y., Wang, K., Zhang, B. Y., Chen, C., Gao, C., and Dong, X. P. (2012) Protein disulfide isomerase regulates endoplasmic reticulum stress and the apoptotic process during prion infection and PrP mutant-induced cytotoxicity. *PLoS One 7*, e38221.

(33) Song, X., Shi, Q., Liu, Z., Wang, Y., Wang, Y., Song, E., and Song, Y. (2016) Unpredicted Downregulation of RAD51 Suggests Genome Instability Induced by Tetrachlorobenzoquinone. *Chem Res Toxicol 29*, 2184-2193.

(34) Song, X., Li, L., Shi, Q., Lehmler, H. J., Fu, J., Su, C., Xia, X., Song, E., and Song, Y. (2015) Polychlorinated Biphenyl Quinone Metabolite Promotes p53-Dependent DNA Damage Checkpoint Activation, S-Phase Cycle Arrest and Extrinsic Apoptosis in Human Liver Hepatocellular Carcinoma HepG2 Cells. *Chem Res Toxicol 28*, 2160-2169.

(35) Uehara, T., Nakamura, T., Yao, D., Shi, Z. Q., Gu, Z., Ma, Y., Masliah, E., Nomura, Y., and Lipton, S. A. (2006) S-nitrosylated protein-disulphide isomerase links protein misfolding to neurodegeneration. *Nature 441*, 513-517.

(36) Song, Y., Wagner, B. A., Witmer, J. R., Lehmler, H. J., and Buettner, G. R. (2009) Nonenzymatic displacement of chlorine and formation of free radicals upon the reaction of glutathione with PCB quinones. *Proc Natl Acad Sci U S A 106*, 9725-9730.

(37) Leber, B., Lin, J., and Andrews, D. W. (2007) Embedded together: the life and death consequences of interaction of the Bcl-2 family with membranes. *Apoptosis 12*, 897-911.

(38) Nie, C., Tian, C., Zhao, L., Petit, P. X., Mehrpour, M., and Chen, Q. (2008) Cysteine 62 of Bax is critical for its conformational activation and its proapoptotic activity in response to H2O2-induced apoptosis. *J Biol Chem 283*, 15359-15369.

(39) Su, C., Zhang, P., Song, X., Shi, Q., Fu, J., Xia, X., Bai, H., Hu, L., Xu, D., Song, E., and Song, Y. (2015) Tetrachlorobenzoquinone activates Nrf2 signaling by Keap1 cross-linking and ubiquitin translocation but not Keap1-Cullin3 complex dissociation. *Chem Res Toxicol 28*, 765-774.

(40) Wang, X., Olberding, K. E., White, C., and Li, C. (2011) Bcl-2 proteins regulate ER membrane permeability to luminal proteins during ER stress-induced apoptosis. *Cell Death Differ 18*, 38-47.

(41) Forman, M. S., Lee, V. M., and Trojanowski, J. Q. (2003) 'Unfolding' pathways in neurodegenerative disease. *Trends Neurosci 26*, 407-410.

(42) Ahmad, K., Baig, M. H., Mushtaq, G., Kamal, M. A., Greig, N. H., and Choi, I. (2017) Commonalities in biological pathways, genetics, and cellular mechanism between Alzheimer Disease and other neurodegenerative diseases: An in silico-updated overview. *Curr Alzheimer Res*.

(43) Manoharan, S., Guillemin, G. J., Abiramasundari, R. S., Essa, M. M., Akbar, M., and Akbar, M. D. (2016) The Role of Reactive Oxygen Species in the Pathogenesis of Alzheimer's Disease, Parkinson's Disease, and Huntington's Disease: A Mini Review. *Oxid Med Cell Longev 2016*, 8590578.

(44) Wang, X., Thomas, B., Sachdeva, R., Arterburn, L., Frye, L., Hatcher, P. G., Cornwell, D. G., and Ma, J. (2006) Mechanism of arylating quinone toxicity involving Michael adduct formation and induction of endoplasmic reticulum stress. *Proc Natl Acad Sci U S A 103*, 3604-3609.

(45) Malhotra, J. D., Miao, H., Zhang, K., Wolfson, A., Pennathur, S., Pipe, S. W., and Kaufman, R. J. (2008) Antioxidants reduce endoplasmic reticulum stress and improve protein secretion. *Proc Natl Acad Sci U S A 105*, 18525-18530.

(46) Santos, C. X., Tanaka, L. Y., Wosniak, J., and Laurindo, F. R. (2009) Mechanisms and implications of reactive oxygen species generation during the unfolded protein response: roles of endoplasmic reticulum oxidoreductases, mitochondrial electron transport, and NADPH oxidase. *Antioxid Redox Signal 11*, 2409-2427.

(47) Lame, M. W., Jones, A. D., Wilson, D. W., and Segall, H. J. (2003) Protein targets of 1,4-benzoquinone and 1,4-naphthoquinone in human bronchial epithelial cells. *Proteomics 3*, 479-495.

(48) Hetz, C., and Mollereau, B. (2014) Disturbance of endoplasmic reticulum proteostasis in neurodegenerative diseases. *Nat Rev Neurosci 15*, 233-249.

(49) Laurindo, F. R., Pescatore, L. A., and Fernandes Dde, C. (2012) Protein disulfide isomerase in redox cell signaling and homeostasis. *Free Radic Biol Med 52*, 1954-1969.

(50) Amanso, A. M., Debbas, V., and Laurindo, F. R. (2011) Proteasome inhibition represses unfolded protein response and Nox4, sensitizing vascular cells to endoplasmic reticulum stress-induced death. *PLoS One 6*, e14591.

(51) Ramachandran, N., Root, P., Jiang, X. M., Hogg, P. J., and Mutus, B. (2001) Mechanism of transfer of NO from extracellular S-nitrosothiols into the cytosol by cell-surface protein disulfide isomerase. *Proc Natl Acad Sci U S A 98*, 9539-9544.

(52) Walker, A. K., Farg, M. A., Bye, C. R., McLean, C. A., Horne, M. K., and Atkin, J. D. (2010) Protein disulphide isomerase protects against protein aggregation and is S-nitrosylated in amyotrophic lateral sclerosis. *Brain 133*, 105-116.

(53) Laurindo, F. R., Araujo, T. L., and Abrahao, T. B. (2014) Nox NADPH oxidases and the endoplasmic reticulum. *Antioxid Redox Signal 20*, 2755-2775.

(54) Soares Moretti, A. I., and Martins Laurindo, F. R. (2017) Protein disulfide isomerases: Redox connections in and out of the endoplasmic reticulum. *Arch Biochem Biophys 617*, 106-119.

(55) Haynes, C. M., and Ron, D. (2010) The mitochondrial UPR - protecting organelle protein homeostasis. *J Cell Sci 123*, 3849-3855.

(56) Hori, O., Ichinoda, F., Tamatani, T., Yamaguchi, A., Sato, N., Ozawa, K., Kitao, Y., Miyazaki, M., Harding, H. P., Ron, D., Tohyama, M., D, M. S., and Ogawa, S. (2002) Transmission of cell stress from endoplasmic reticulum to mitochondria: enhanced expression of Lon protease. *J Cell Biol 157*, 1151-1160.

(57) Hetz, C., Bernasconi, P., Fisher, J., Lee, A. H., Bassik, M. C., Antonsson, B., Brandt, G. S., Iwakoshi, N. N., Schinzel, A., Glimcher, L. H., and Korsmeyer, S. J. (2006) Proapoptotic BAX and BAK modulate the unfolded protein response by a direct interaction with IRE1alpha. *Science 312*, 572-576.

(58) Eletto, D., Eletto, D., Dersh, D., Gidalevitz, T., and Argon, Y. (2014) Protein disulfide isomerase A6 controls the decay of IRE1alpha signaling via disulfide-dependent association. *Mol Cell 53*, 562-576.

Table 1: Sequence of all siRNA used in RNA interference experiment.

Gene	Sense (5'-3')	Antisense (5'-3')
PDIA1-1	GCAAGAUCCUGUUCAUCUUTT	AAGAUGAACAGGAUCUUGCTT
PDIA1-2	GGUCCUCUUUAAGAAGUUUTT	AAACUUCUUAAAGAGGACCTT
PDIA1-3	GGCAAAUUGAGCAACUUUATT	UAAAGUUGCUCAAUUUGCCTT
PDIA3-1	GGAAUAGUCCCAUUAGCAATT	UUGCUAAUGGGACUAUUCCTT
PDIA3-2	CCAGCAACUUGAGAGAUAATT	UUAUCUCUCAAGUUGCUGGTT
PDIA3-3	CCAACGAAGGACCUGUCAATT	UUGACAGGUCCUUCGUUGGTT

Table 2: Sequence of all primers used in RT-qPCR experiment.

`	Sequences (5'-3')	
ATF4	Forward	CTTCTCCAGGTGTTCCTCGT
	Reverse	TGCTCAGCCCTCTTCTTCTG
CHOP	Forward	AAGAATCAAAAACCTTCACTACTCTTGACC
	Reverse	TGGGAGGTGCTTGTGACCTCTGC
XBP-1s	Forward	GAGTCCGCAGCAGGTG
	Reverse	GCGTCAGAATCCATGGGA
β-actin	Forward	AGTGTGACGTTGACATCCGT
	Reverse	GACTGATCGTACTCCTGCTT
XBP-1	Forward	AAACAGAGTAGCAGCGCAGACTGC
(for RT-PCR)	Reverse	GGATCTCTAAAACTAGAGGCTTGGTG
GAPDH	Forward	TGGCACAGTCAAGGCTGAGA
(for RT-PCR)	Reverse	CTTCTGAGTGGCAGTGATGG

Figure Legends

Figure 1. Effects of TCBQ on ER stress in PC12 cells. Cells were treated with 0, 5, 10, 15 or 20 μM TCBQ for 24 hr. **(A)** Effects of TCBQ on IRE1α phosphorylation and activation of JNK signaling pathway. Total proteins were harvested and subjected to Western blotting of the indicated proteins. **(B)** Effect of TCBQ on XBP-1 splicing (XBP1s). *upper panel,* after 24 hr treatment, total mRNA was extracted. Then real-time PCR was conducted to detect XBP-1 mRNA splicing. The amplified product was resolved using 7.5% SDS-PAGE. *lower panels,* XBP-1s mRNA expression was measured by RT-qPCR. **(C)** Effect of TCBQ on ATF6 pathways. The expression of ATF6 and cleaved ATF6 were performed by Western blotting. TCBQ increased mRNA levels of ATF4 **(D)** and CHOP **(E)**. ATF4 and CHOP mRNA expression were determined by RT-qPCR. Activation of caspase 12 **(F)** and effect of intracellular Ca^{2+} **(G)** after TCBQ exposure**.** After incubated with different concentrations of TCBQ for 24 hr, cells were loaded with Fura-2/AM, and then $[Ca^{2+}]_i$ was monitored as described in "Materials and Methods". The bar graphs shown in the figure were expressed as the means ± SD of three independent experiments with similar results. β-Actin was used as a housekeeping gene in above experiments. ***p<0.001 compared with the untreated control.

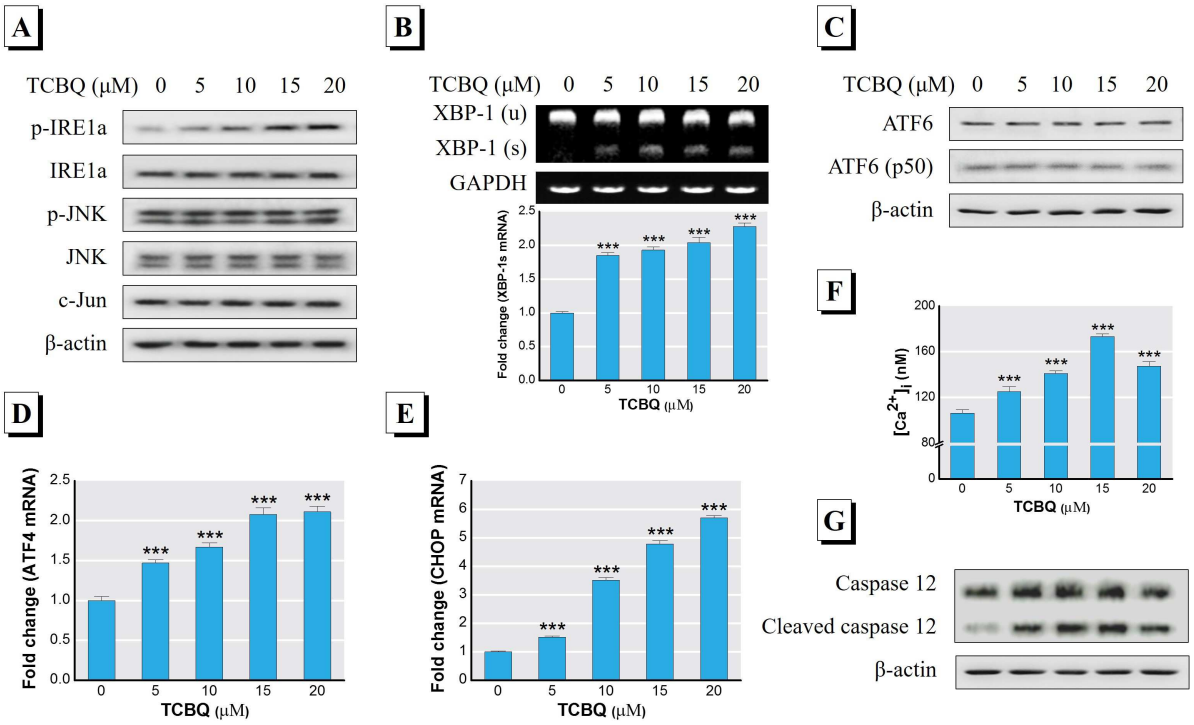
A
TCBQ (μM) 0 5 10 15 20
p-IRE1a
IRE1a
p-JNK
JNK
c-Jun
β-actin
B
TCBQ (μM) 0 5 10 15 20
XBP-1 (u)
XBP-1 (s)
GAPDH
Fold change (XBP-1s mRNA)
TCBQ (μM)
C
TCBQ (μM) 0 5 10 15 20
ATF6
ATF6 (p50)
β-actin
D
Fold change (ATF4 mRNA)
TCBQ (μM)
E
Fold change (CHOP mRNA)
TCBQ (μM)
F
[Ca2+]i (nM)
TCBQ (μM)
G
Caspase 12
Cleaved caspase 12
β-actin

Figure 2. PDIA1 and PDIA3 were involved in the neurotoxicity of TCBQ in PC12 cells. Inhibiting PDI catalytic activities affected the apoptosis induced by TCBQ. Cells were pretreated with or without 10 or 20 μM securinine **(A)**, 15 or 30 μM thiomuscimol **(B)**, 50 or 100 μM bacitracin **(C)**, respectively, and then incubated with TCBQ for 24 hr. Cell viability was determined using CCK-8 assay. **(D)** siRNA knockdown of PDIA1 and confirmation the role of PDIA1 in TCBQ-induced apoptosis. Each siRNA was used in two concentrations for different degrees of knockdown PDIA1 protein, so that the function of PDIA1 protein was fully verified. Graph revealed the rescue of cell viability by PDIA1 siRNA following a 48 hr knockdown and 24 hr treatment with TCBQ. **(E)** The parallel analysis was performed to confirm the function of PDIA3. The original cell viability statistics were shown in Supplemental Material, Figure S**4**. Data from three independent experiments were expressed as the means ± SD. $^{*}p<0.05$, $^{**}p<0.01$, $^{***}p<0.001$ compared with the 10 μM TCBQ group. $^{\#}p<0.05$, $^{\#\#}p<0.01$, $^{\#\#\#}p<0.001$ compared with the 20 μM TCBQ group.

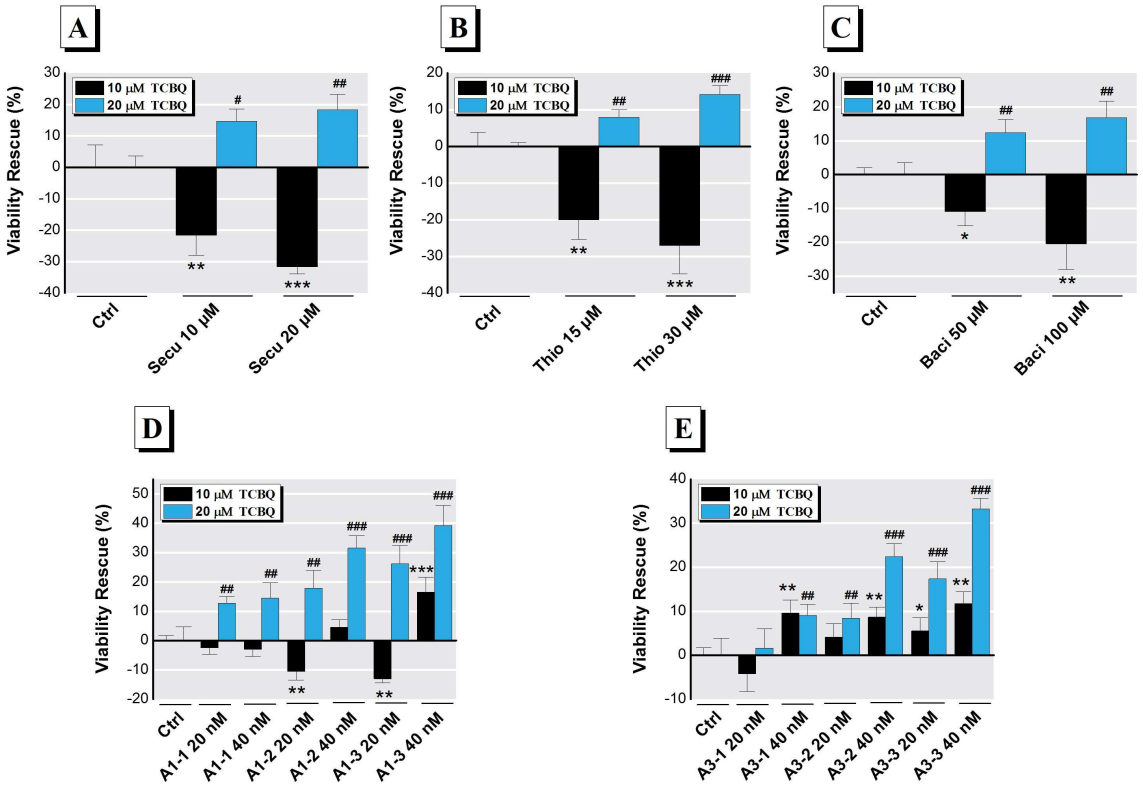
A
B
C
D
E
10 μM TCBQ
20 μM TCBQ
Viability Rescue (%)
Ctrl
Secu 10 μM
Secu 20 μM
Thio 15 μM
Thio 30 μM
Baci 50 μM
Baci 100 μM
A1-1 20 nM
A1-1 40 nM
A1-2 20 nM
A1-2 40 nM
A1-3 20 nM
A1-3 40 nM
A3-1 20 nM
A3-1 40 nM
A3-2 20 nM
A3-2 40 nM
A3-3 20 nM
A3-3 40 nM

Figure 3. Effects of TCBQ on the expression and modification of PDI proteins. Expression of PDIA1 **(A)** or PDIA3 **(B)** had no obvious change in PC12 cells incubated with increasing concentrations of TCBQ for 24 hr. Western blotting was performed to detect PDIs expression. Lower graphs showed the values for densitometric analysis of each spot and expressed as PDIs/β-actin ratio. **(C)** Effect of TBCQ on SNO-PDIs formation. PC12 cells were stimulated with TCBQ for 24 hr or 100 μM GSNO for 30 min as a positive control. One half of the lysate was to evaluate SNO-PDIs formation using a biotin-switch assay, the other half was used to detect total amount of PDIA1 and β-actin. **(D)** Effect of SNO-PDIs formation by prior treatment with TCBQ. PC12 cells were pre-incubated with different concentrations of TCBQ for 24 hr and then treatment with or without 100 μM GSNO for 30 min.

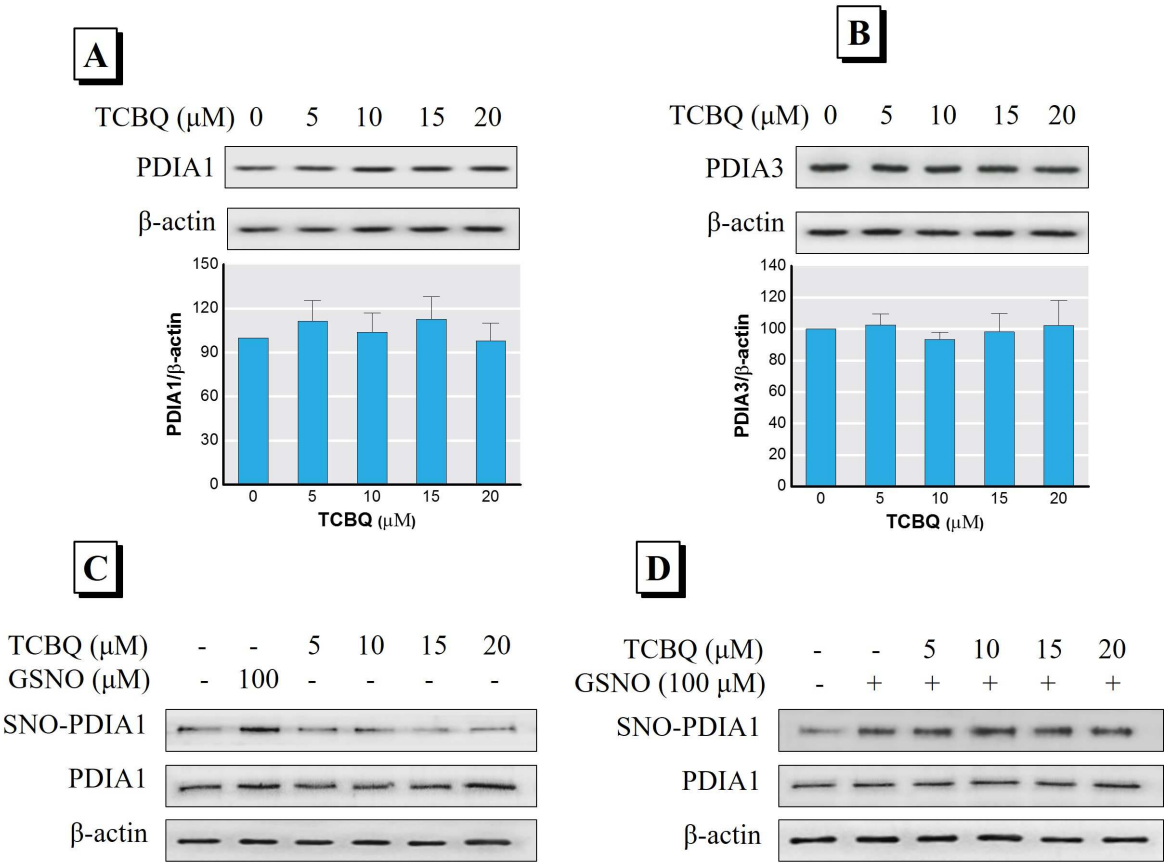

Figure 4. Effects of TCBQ on subcellular localization of PDIs and MOMP. **(A)** After treatment with different concentrations of TCBQ for 24 hr, Western blotting and protein quantification of PDIs in the cytosolic, mitochondrial, and ER-microsomal cell fractions were performed (normalized to β-actin, COX IV and calnexin, respectively). **(B)** TCBQ changed the distribution of PDIA1. Immunofluorescence staining of the PDIA1 (green) and calnexin (red) distribution in PC12 cells. Cells were treated with or without 20 μM TCBQ for 24 hr and all nuclei were stained with DAPI (blue), magnification, ×1000; bars = 10 μm. **(C)** Effect of TCBQ on mitochondrial release of cytochrome *c*. The cells were treated with TCBQ, then Western blotting was performed after removal of mitochondria and ER. **(D)** Knockdown of PDIA1 and PDIA3 protected cells from TCBQ-induced MOMP. PDIA1 and PDIA3 expression was limiting knockdown by 40 nM siRNA A1-3 and A3-3, respectively. Then cells were stimulated with 20 μM TCBQ for 24 hr. Mitochondrial release of cytochrome *c* and smac were determined. PDIs siRNA suppressed mitochondrial cytochrome *c* and smac release. **(E)** Mitochondrial membrane depolarization induced by TCBQ was suppressed by PDI inhibitors. Cells were pretreated with thiomuscimol or securinine, and then incubated with TCBQ for 24 hr. Images shown were representative observations from three independent experiments. Green fluorescence represented JC-1 monomer with low MMP. Red staining represented JC-1 aggregate with high MMP. MMP damage was indicated by a shift from red fluorescence to green fluorescence, magnification, ×200; bars = 50 μm. Data from three independent experiments were expressed as the means ± SD. $^{**}p<0.01$, $^{***}p<0.001$ compared with the untreated control.

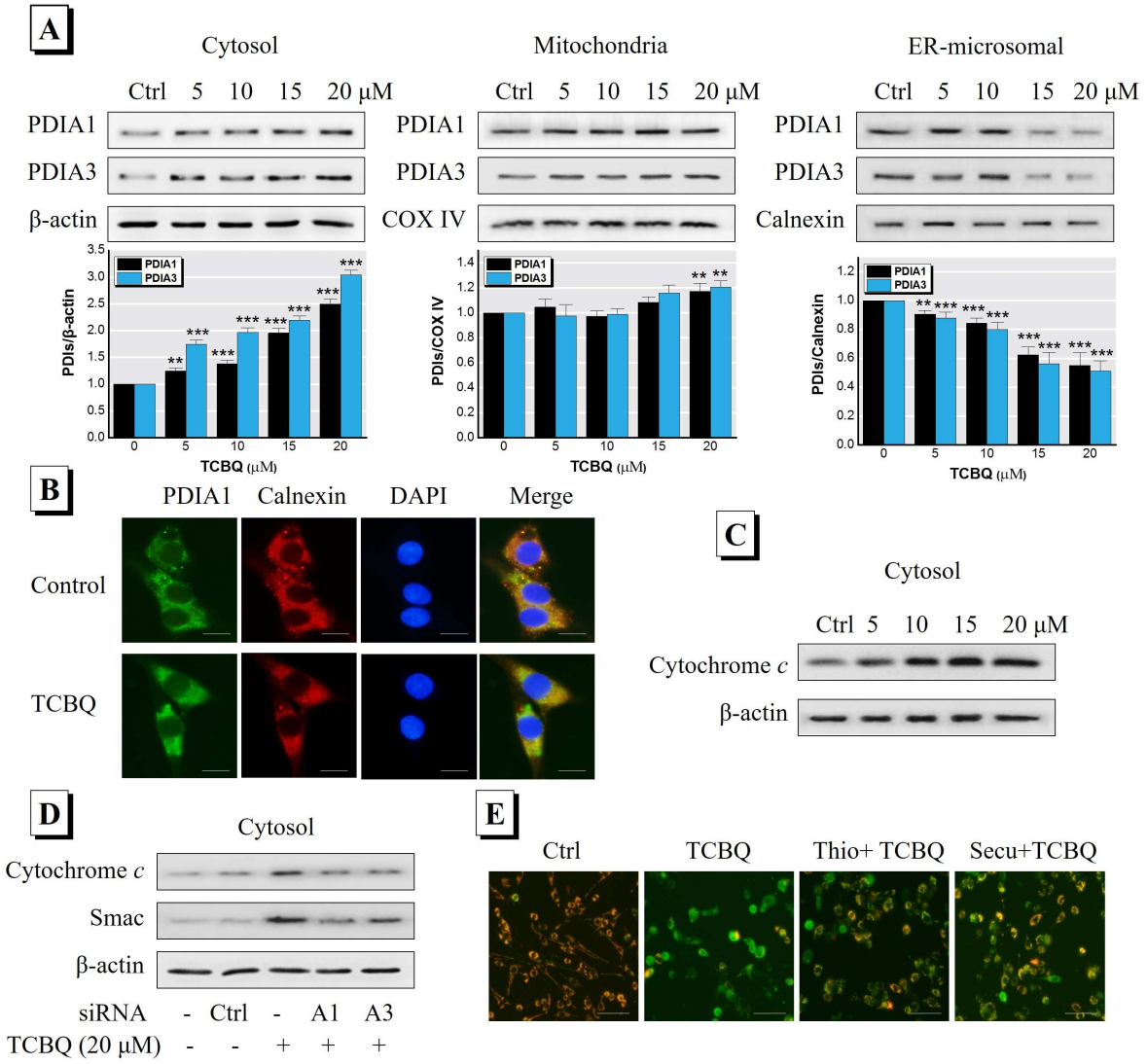
A
Cytosol
Mitochondria
ER-microsomal
Ctrl 5 10 15 20 μM
PDIA1
PDIA3
β-actin
COX IV
Calnexin
PDIs/β-actin
PDIs/COX IV
PDIs/Calnexin
TCBQ (μM)
B
PDIA1 Calnexin DAPI Merge
Control
TCBQ
C
Cytosol
Ctrl 5 10 15 20 μM
Cytochrome c
β-actin
D
Cytosol
Cytochrome c
Smac
β-actin
siRNA - Ctrl - A1 A3
TCBQ (20 μM) - - + + +
E
Ctrl
TCBQ
Thio+ TCBQ
Secu+TCBQ

Figure 5. Involvement of PDIA1 and PDIA3 in TCBQ-mediated Bcl-2 protein family oligomerization in mitochondria. **(A)** Effect of TCBQ on Bak oligomerization. PDIA1 and PDIA3 expression were limiting knockdown by 40 nM siRNA A1-3 and A3-3, respectively, then cells were stimulated with 20 μM TCBQ for 24 hr. Mitochondria were isolated as described in "Materials and Methods", then cross-linking was performed by adding bis(maleimido)hexane. Cytosolic fractions and mitochondria lysates were subjected to Western blotting (normalized to β-actin and COX IV, respectively). Bak-M, Bak-D and Bak-T represented Bak monomer, dimer and trimer, respectively. **(B)** Effect of TCBQ on Bax oligomerization. Western blotting for mitochondrial and cytosolic Bax protein following treatment as above. Bax protein did not became oligomerized in mitochondria during TCBQ-induced MOMP. Bax-M represented Bax monomer. P, pellet, mitochondrial fraction; S, supernatant, cytosolic fraction.

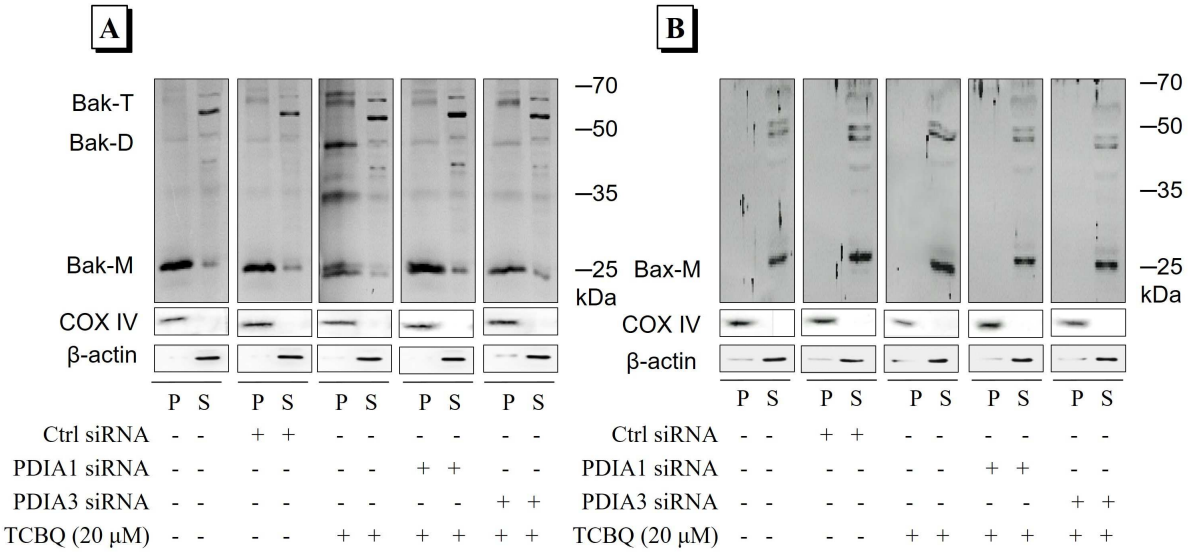

Figure 6. ROS Generation Play an essential role on PDIs Translocation and Pro-death. **(A)** Effect of NAC or 4-PBA on TCBQ-induced PDIs accumulation in the cytosol. Cells were pretreated with 5 mM NAC or 5 mM 4-PBA for 1 hr and then exposed to 20 μM TCBQ for 24 hr. Western blotting test was performed after removal of mitochondria and endoplasmic reticulum. **(B)** TUNEL staining. Cells were pretreated with 5 mM NAC for 1 hr and then exposed to 20 μM TCBQ for 24 hr. The apoptotic cells were detected by immunofluorescent staining with TUNEL(red). DAPI (blue) staining was used to label the nuclei, magnification, ×200; bars = 50 μm. **(C)** Effect of NAC on cell viability induced by TCBQ. Cell viability was indicated by CCK-8 assay after indicated treatment. **(D)** Effect of NAC on LDH release induced by TCBQ. LDH in the supernatant of the culture medium was measured, which indicated cell injury. Data from three independent experiments were expressed as the means ± SD. ***p <0.001 compared with the untreated control, $^{###}p$<0.001 compared with TCBQ group.

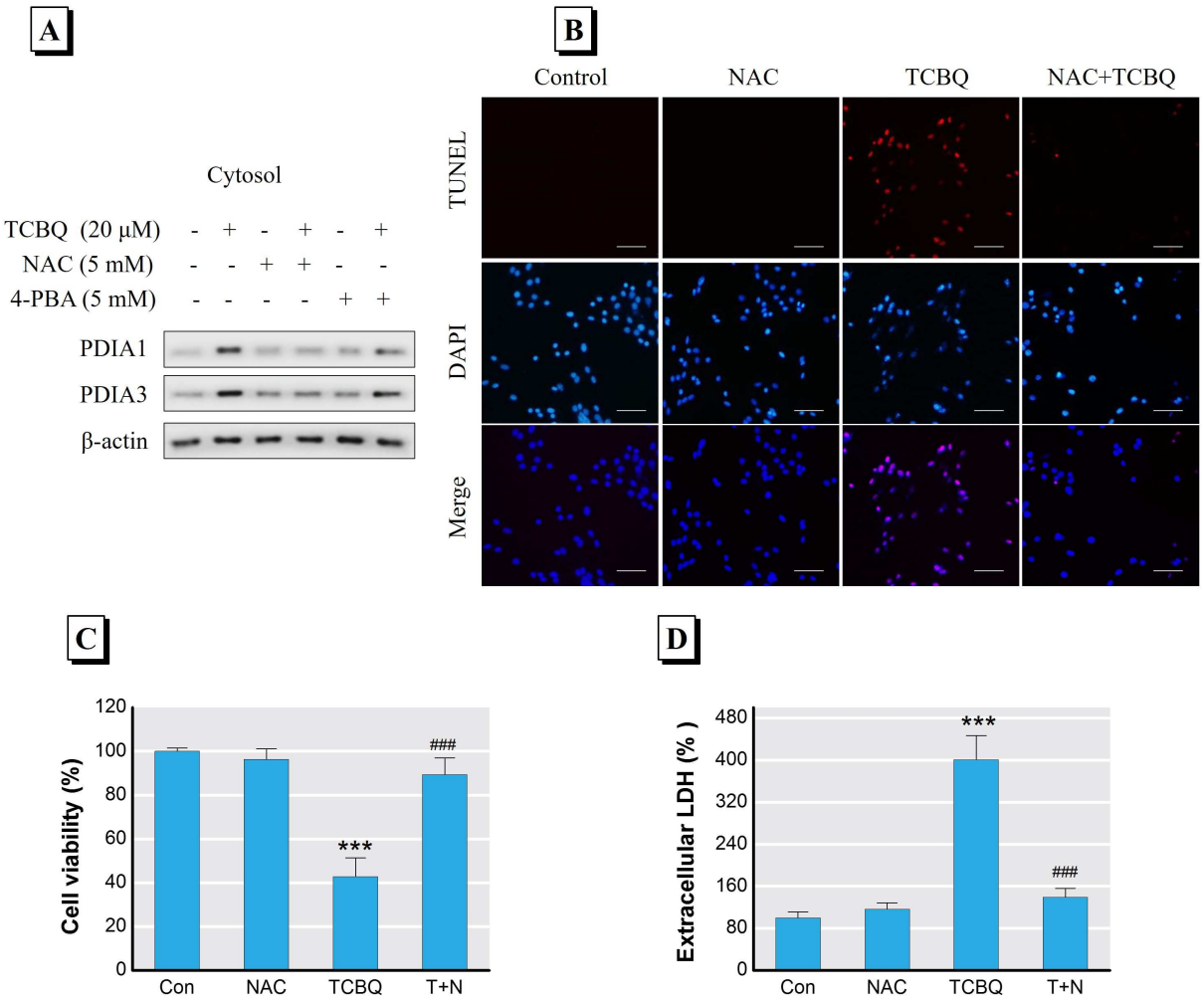
A
Cytosol
TCBQ (20 μM) - + - + - +
NAC (5 mM) - - + + - -
4-PBA (5 mM) - - - - + +
PDIA1
PDIA3
β-actin
B
Control
NAC
TCBQ
NAC+TCBQ
TUNEL
DAPI
Merge
C
Cell viability (%)
120
100
80
60
40
20
0
***
###
Con
NAC
TCBQ
T+N
D
Extracellular LDH (%)
480
400
320
240
160
80
0
***
###
Con
NAC
TCBQ
T+N